Detection of nucleic acids *in situ*: novel oligonucleotide analogues for target-assembled DNA-mounted exciplexes

Elena V. Bichenkova,* Abdul Gbaj, Lindsey Walsh, Hannah E. Savage, Candelaria Rogert,† Ali R. Sardarian,‡ Laura L. Etchells and Kenneth T. Douglas*

This research describes the effects of structural variation and medium effects for the novel split-oligonucleotide (tandem) probe systems for exciplex-based fluorescence detection of DNA. In this approach the detection system is split at a molecular level into signal-silent components, which must be assembled correctly into a specific 3-dimensional structure to ensure close proximity of the exciplex partners and the consequent exciplex fluorescence emission on excitation. The model system consists of two 8-mer oligonucleotides, complementary to adjacent sites of a 16-mer DNA target. Each probe oligonucleotide is equipped with functions able to form an exciplex on correct, contiguous hybridization. This study investigates the influence of a number of structural aspects (*i.e.* chemical structure and composition of exciplex partners, length and structure of linker groups, locations of exciplex partner attachment, as well as effects of media) on the performance of DNA-mounted exciplex systems. The extremely rigorous structural demands for exciplex formation and emission required careful structural design of linkers and partners for exciplex formation, which are here described. Certain organic solvents (especially trifluoroethanol) specifically favour emission of the DNA-mounted exciplexes, probably the net result of the particular duplex structure and specific solvation of the exciplex partners. The exciplexes formed emitted at ∼480 nm with large Stokes shifts (∼130–140 nm). Comparative studies with pyrene excimer systems were also carried out.
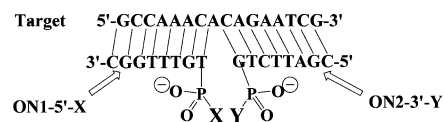
Introduction§

Detection of specific target nucleic acid sequences is commonly achieved by hybridization of a fluorescently labelled oligonucleotide probe to a complementary target. This usually has very large background fluorescence when one compares the same fluorophore-labelled oligonucleotide in its single-stranded and duplex-bound forms.[1] It is possible to decrease the background fluorescence by using two short oligonucleotide probes that are complementary to neighbouring sites of the same DNA target, and can form a pyrene excimer (X = Y = pyrene in Fig. 1). Excitation of one of the pyrene partners, forms an excited state dimer (excimer) that emits at long wavelength (Stokes shifts >100 nm).[2–8] Thus, the target assembles its own detector from components which are non-fluorescent at the detection wavelength, giving a massive improvement in terms of the reduced background.

Fig. 1 Schematic diagram of DNA-mounted exciprobes. ON1-5′-X and ON2-3′-Y represent oligonucleotide split-probes with covalently attached exciplex partners X and Y, respectively. The oligonucleotide parts of the split-probes ON1 and ON2 possess sequences 5′-pdTGTTTGGC and dCGATTCTG-3′p, respectively. GCCAAACACAGAATC is the target DNA. Structural variants of the exciprobes tested, along with nomenclature, are shown in Table 1.

For excimer–DNA systems, X and Y must be identical. More variety in the molecular properties of such systems and hence their potential applications would be possible if X and Y could be different from each other and could be varied (*i.e.* exciplexes),[9,10] which provides a clear advantage for exciplex-based detecting systems over excimer-based analogues. Being able to vary the chemical and physical natures of X and Y should allow exciplex-assembling systems of a range of properties to be constructed increasing their potential for applications, for example, tuning of properties to provide detectors matched to specific needs, or possibly for multiplexing. In model organic intramolecular systems corresponding to those exciplex partners used in this DNA system, the wavelengths of exciplex emission were strongly affected by the identities of X and Y.[11] To achieve efficient exciplex or excimer formation, the partners X and Y must be able to approach

Wolfson Centre for Rational Structure-Based Design of Molecular Diagnostics, School of Pharmacy and Pharmaceutical Sciences, University of Manchester, Manchester, M13 9PL, UK. E-mail: elena.bichenkova@manchester.ac.uk; Fax: +44 161 275 2481; Tel: +44 161 275 8359
† Present address: Solexa Ltd, Chesterford Research Park, Little Chesterford, Essex, CB10 1XL, UK.
‡ Present address: Department of Chemistry, Shiraz University, Shiraz, Iran.

§ Abbreviations used: BOP, benzotriazol-1-yloxytris(dimethylamino)-phosphonium; I_E/I_M, ratio of exciplex or excimer fluorescence intensity to that of the corresponding locally excited state for the pyrene or perylene component of the system; LES, locally excited state; ON1, oligonucleotide 1 (5′pdTGTTTGGC); ON2, oligonucleotide 2 (dCGATTCTG3′p); ou_{260}, the amount of oligonucleotide that gives an optical density of 1 at 260 nm for a 1 cm pathlength; SNP, single nucleotide polymorphism; λ_{ext}, excitation wavelength maximum; λ_{em}, wavelength emission maximum.

each other very closely (typically the distance is ∼4 Å for the pyrene excimer[9,10]). This distance is of the order of the thickness of a base pair. Thus, the potential resolution of the exciplex or excimer systems theoretically approaches a single base pair. In contrast, FRET systems are effective over much greater distances (10–100 Å; >∼3 bp) and hence of low resolution.

While excimer-based systems have been successfully applied to nucleic acid detection,[3,5,7,8,12] exciplex-based split-probe systems have been introduced only recently and studied to a much lesser extent.[1,13,14] There are several differences[15] in the fundamental natures of excimers and exciplexes. The most problematic difference in terms of DNA detection is the much greater solvent sensitivity of exciplexes compared to excimers. For solvents of polarity greater than approximately that of acetonitrile intramolecular organic exciplex emission is usually totally quenched,[16–25] although there are some exceptions,[26,27] and very recently we described an organic intramolecular exciplex system that emits even in solvents with a dielectric constant of over 180.[11] Recently Kashida *et al.*[14] reported exciplex emission in aqueous solution from pyrene and *N*,*N*-dimethylaniline moieties incorporated into the middle of DNA probes with the exciplex partners directed internally and lying in the centre of a (distorted) duplex. This approach allowed successful detection of one-base deletion in DNA sequences, but as it requires formation of specific secondary structures (*e.g.* loops), the unambiguous signalling of single base changes has not yet been reported for it. We have introduced an alternative approach,[1,13] which utilised two separate oligonucleotide split-probes, each equipped with exciplex partners that are oriented towards the bulk medium. We also reported assay conditions[1,13] under which DNA-based exciplexes can be strongly emissive for systems constructed according to the design of Fig. 1, and allow the clean detection of single base mismatches and thus the potential for SNP calling. However, only one initial prototype pair of exciplex partners was described in detail.[13] Thus, we now report the influence of a number of structural aspects (*i.e.* chemical structure and composition of exci-partners, length and structure of linker groups, locations of exci-partner attachment, as well as effects of media) on the performance of DNA-mounted exciplex systems conceptualised as in Fig. 1. The 16-mer-target nucleotide sequence (Fig. 1) was chosen to avoid formation of secondary structure. The exciplex is formed between various donor and acceptor moieties (see Table 1 for structures) covalently attached to the 5′- and 3′-terminal phosphate groups, respectively, of the 8-mer oligonucleotides shown in Fig. 1 (referred to as the probe oligonucleotides or exciprobes). The structures and nomenclature used for the systems studied are shown in Fig. 1 and Table 1.

Results

Split-probe system in aqueous solutions

Split-probe systems SP-1–SP-41 (Table 1) were constructed using appropriate combinations of potential exciplex-forming oligonucleotide-probe components ON1-5′-X and ON2-3′-Y mixed with 16-mer target in 0.01 M Tris buffer (pH 8.3), containing 0.1 M NaCl at 10 °C. In the absence of target, mixing equimolar amounts of two exciprobe components ON1-5′-X and ON2-3′-Y (2.5 μM) did not alter λ_{max} for emission or excitation of the components, indicating no interaction between the probes in the

absence of target. Adding the target strand led to strong quenching of the pyrene emission (LES), and λ_{max} for emission shifted from 340 nm to higher wavelength (typically by 3–7 nm). This evidence of hybridisation in the full duplex tandem system was confirmed by the A_{260} melting profiles.[13] However, none of the potential exciplex systems studied showed exciplex emission in such purely aqueous conditions, although excimer emission at ∼480 nm was observed for SP-1 under identical conditions (Fig. 2).
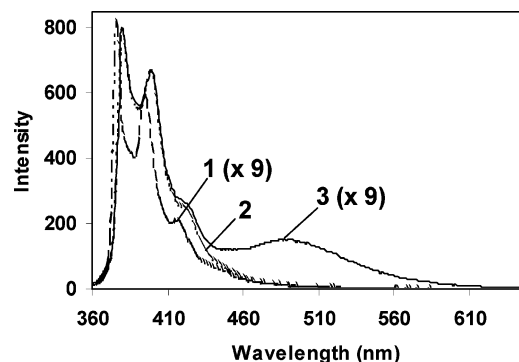
Fig. 2 Fluorescence spectra of the excimer-forming SP-1 system at different stages of self-assembly in pure aqueous solution. **1**, ON1-5′-Pyr probe alone; **2**, ON1-5′-Pyr + ON2-3′-Pyr; **3**, fully assembled SP-1 system (ON1-5′-Pyr + ON2-3′-Pyr + Target). Spectra were recorded at 5 °C in 10 mM Tris buffer, pH 8.3, 0.1 M NaCl (λ_{ext} 345 nm, slitwidth 3). Spectra **1** and **3** were re-scaled to the 380 nm pyrene LES emission band in spectrum **2** using a scaling factor of 9. The intensity of the pyrene (LES) peaks for systems with a 3′-pyrene label is usually very much greater than for similar systems with the pyrene on a 5′-site. For this reason the intensity observed for system **2** (which contains a 3′- as well as a 5′-pyrene-labelled probe, mutually non-interacting) is much greater than for system **1** with only a 5′-pyrene probe present in solution, and it was useful to scale the data.
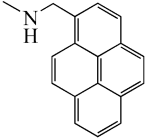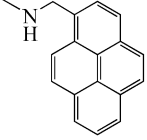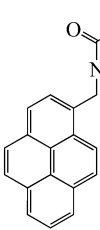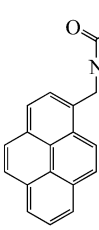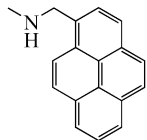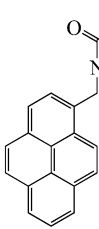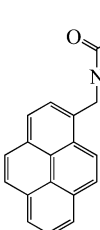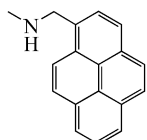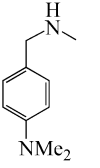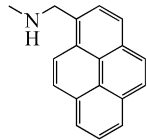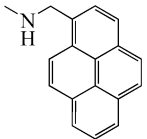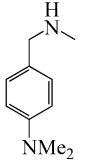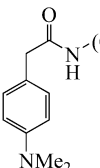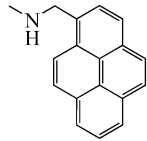
Influence of co-solvents on exciplex signals from split-probe oligo systems

Exciplex emission was specifically enhanced by trifluoroethanol (TFE).[13] Fig. 3 (curve 1) shows the emission spectrum of the
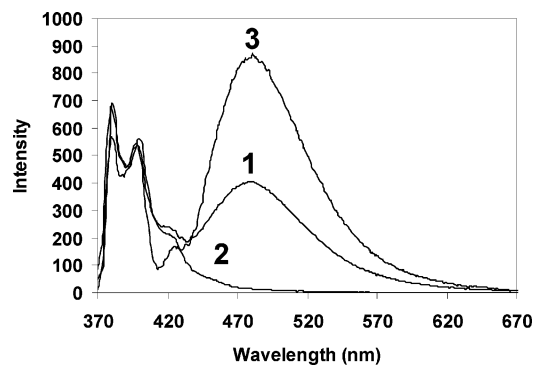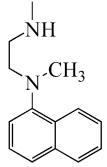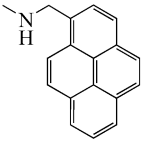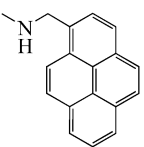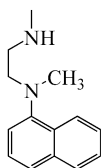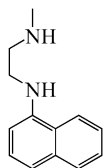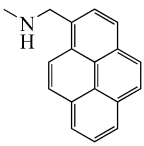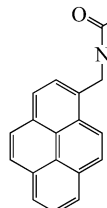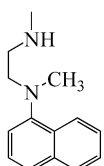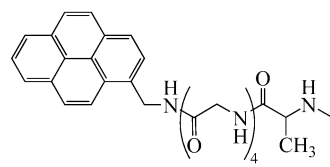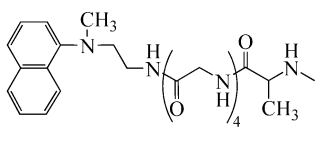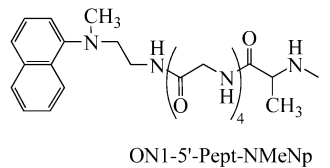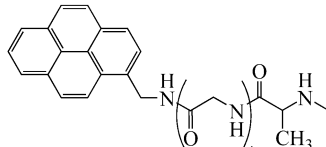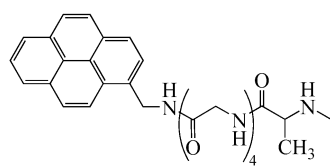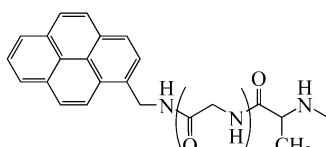
Fig. 3 Fluorescence spectra of the SP-19 split-probe system (**1**) and a control system (ON1-5′-Pyr + ON2 + target) with unmodified ON2 oligo-probe lacking the *N*,*N*′-dimethylnaphthalene exci-partner (**2**) recorded at 10 °C. Spectrum (**3**) is the emission spectrum of re-annealed SP-19 system following a heating–re-cooling cycle. Spectra were recorded in Tris buffer (10 mM Tris, pH 8.3, 100 mM NaCl) containing 80% TFE v/v (excitation at 350 nm).

Table 1 Structures and nomenclature of modified oligonucleotides used

Code	Exci-partner X (to give ON1-5′-X exciprobe)	Exci-partner Y (to give ON2-3′-Y exciprobe)
Excimer systems SP-1	ON1-5'-Pyr	ON2-3'-Pyr
SP-25	ON1-5'-AspPyr	ON2-3'-AspPyr
SP-40	ON1-5'-Pyr	ON2-3'-AspPyr
SP-41	ON1-5'-AspPyr	ON2-3'-Pyr
Exciplex systems SP-2	ON1-5'-DMA	ON2-3'-Pyr
SP-4	ON1-5'-Pyr	ON2-3'-DMA
SP-3	ON1-5'-C7DMA	ON2-3'-Pyr

Table 1 (*Contd.*)

Code	Exci-partner X (to give ON1-5′-X exciprobe)	Exci-partner Y (to give ON2-3′-Y exciprobe)
SP-18	ON1-5'-NMeNp	ON2-3'-Pyr
SP-19	ON1-5'-Pyr	ON2-3'-NMeNp
SP-20	ON1-5'-NHNp	ON2-3'-Pyr
SP-26	ON1-5'-AspPyr	ON2-3'-NMeNp
SP-27	ON1-5'-Pept-Pyr	ON2-3'-Pept-NMeNp
SP-28	ON1-5'-Pept-NMeNp	ON2-3'-Pept-Pyr
SP-29	ON1-5'-Pept-Pyr	ON2-3'-Pept-Pyr

SP-19 split-probe exciplex system (ON1-5′Pyr + ON2-3′NMeNp + target strand) recorded at 10° C in Tris buffer containing 80% TFE. As in fully aqueous solutions, on hybridisation of probes to target there was a bathochromic shift and quenching of the pyrene LES emission. The new, broad emission band at ~480 nm (Fig. 3) in the presence of target strand at 80% TFE is attributable to exciplex formation between the pyrenyl and dialkylnaphthyl exci-partners. A control experiment (curve 2) under identical

1042 | *Org. Biomol. Chem.*, 2007, **5**, 1039–1051

This journal is © The Royal Society of Chemistry 2007

conditions, but without an *N,N*-dialkylaminonaphthaleno exci-partner at the 3′-terminal phosphate group of ON2 (leaving a free 3′-phosphate), revealed no exciplex emission at 480 nm, although there was quenching and red shift of the LES emission, indicating hybridisation of the probes with the target. Thus, the 480 nm emission band was attributed to interaction between the two exci-partners, not interaction of the exci-partner(s) with the nucleotide bases. An additional control experiment of mixing the two oligo probes in the absence of the target DNA sequence (data not shown) resulted in no exciplex emission at 480 nm, demonstrating that tandem hybridisation to the target is necessary for the exciplex signal development.

A heating–re-cooling cycle can significantly improve the exci-plex signal (Fig. 3, curve 3). Heating the system (up to 70 °C) results in duplex melting and subsequent separation of exciplex partners, which causes the exciplex band to disappear (accompanied by an increase in LES emission intensity and λ_{em} shifting back to that for the ON1-5′Pyr probe). On cooling back to 10 °C the oligonucleotide chains re-anneal and the full tandem system reassembles with concomitant exciplex emission of greater intensity than before the heating–re-cooling cycle. The increased intensity is likely to be the result of thermodynamically achieving a tandem duplex conformation with more favourable orientations of the exci-partners. This phenomenon was observed for various split-probe systems and assigned to improved mutual orientation of exci-partners (in terms of exciplex assembly) as a result of the slow cooling. The heating–cooling cycle presumably disrupts undesirable, competitive hydrophobic interactions of the exci-partners with the DNA, freeing them for exciplex formation.

Fig. 4 shows emission spectra of the split-probe exciplex SP-19 system (ON1-5′-Pyr + ON2-3′-NMeNp + target strand) in Tris buffer containing various percentages of TFE (spectra were recorded without heating–re-cooling optimisation). A plot of the effect of percentage TFE on the ratio (I_E/I_M) for SP-19 is shown in the inset to Fig. 4, where I_M is intensity of fluorescence emitted by the pyrene LES at 376 nm and I_E is intensity of the exciplex band at 480 nm. The plot shows that the strongest exciplex emission

occurs once a level of $\geq 80\%$ TFE has been reached. In addition, the maximum wavelength of the excitation spectrum is influenced by a higher percentage of TFE: 340 nm for 70%; 350 nm for 80%; 348 for 85% and 335 nm for 90%. Values of λ_{max} for exciplex emission at various percentages of TFE also varied (Fig. 4) and were (percentages of TFE in parentheses): 465 nm (60%), 483 nm (70%), 482 nm (80%), 480 nm (85%) and 481 nm (90%). The wavelength shift of the excitation spectrum may arise from a simple solvent effect on the excitation spectrum of the exciplex and/or from a structural change in the environment of the exciplex partners with respect to each other and the DNA to which they are chemically bound.

Similar observations were made for the pyrene excimer (SP-1 split-probe system) assembly. Excimer fluorescence at 481 nm increased in intensity relative to the LES peak by means of a heating–re-cooling cycle. For example, in 80% TFE/pH 8.3 Tris medium I_E/I_M changed from 2.24 to 2.74 by heating from 10 °C to 70 °C over 5 minutes followed by cooling back to 10 °C over 15 minutes. In addition, excimer emission for SP-1 was also augmented by the presence of TFE: I_E/I_M values were (percentage of TFE in parentheses): 0.24 (20%), 0.46 (40%), 0.62 (60%) and 2.24 (80%).

Effect of reversing relative locations of donor and acceptor partners

Exciprobe performance can be strongly affected by the relative location of donor and acceptor partners within the oligo probe systems, *i.e.* by their relative attachment sites at the 3′- and 5′-juxtaposed ends of the hybridised short probe oligonucleotides, ON1 and ON2 in Fig. 1. Fig. 5 compares the fluorescence emission spectra for systems SP-19 *vs.* SP-18 (**A**, spectra **1** and **2**, respectively) and SP-4 *vs.* SP-2 (**B**, spectra **3** and **4**, respectively) in which the relative locations of the acceptor partner (pyrene) and the donor (*N,N*-dialkylaminonaphthalene (for SP-18 and SP-19, **A**), or *N,N*-dimethylaminobenzyl (for SP-2 and SP-4, **B**) were reversed. Since the formation of the exciplex/excimer band is accompanied by quenching of the LES signal, I_E/I_M (the ratio between the intensity of the LES pyrene emission and the exciplex/excimer emission) is a good measure of formation of excited state complex/dimer efficiency.[28] As a rule, a higher *exciplex*:*LES* ratio (I_E/I_M) was observed with the pyrenyl group at the 5′-terminal phosphate site of oligo probe ON1 and the electron-donating group (*i.e. N,N*-dialkylaminonaphthalene for SP-19 or *N,N*-dimethylaminobenzyl for SP-4) at the 3′-terminal phosphate site of oligo probe ON2 (spectra 1 and 3, respectively). Changing the relative (3′- or 5′-) locations of the electron donor and acceptor partners to give systems SP-18 and SP-2, respectively, resulted in a decrease in *exciplex*:*LES* ratio (see spectra 2 and 4, respectively).

Effect of structural properties of exci-partners on exciprobe performance

(i) Hydrophobicity and electron-donating properties of the exci-partners. Our experimental data show that based on the relatively crude measure of I_E/I_M, the ability to form an excited state complex decreases in the order pyrene > *N,N*-dialkylamino-naphthalene > *N,N*-dimethylaminobenzyl, if the second exciplex partner is represented by a fixed aromatic group (*e.g.* pyrenyl). Fig. 6A contrasts the emission spectra of SP-1, SP-4 and SP-19

Fig. 4 Effect of percentage trifluoroethanol (v/v as indicated on the spectra labels) on exciplex emission for the SP-19 system. Spectra were recorded at 5 °C with component concentrations of 2.5 μM in 10 mM Tris, pH 8.3, containing 0.1 M NaCl and percentage of TFE as indicated by labels; λ_{ext} 350 nm, slit width 5 nm. Spectra were base-line corrected for small contributions from buffer- and co-solvent background. The inset shows a plot of the ratio of exciplex fluorescence to LES fluorescence (I_E/I_M) *versus* percentage TFE (v/v).

Fig. 5 Comparison of the fluorescence emission of exciplex-forming systems SP-19 *vs.* SP-18 (**A**, spectra **1** and **2**, respectively) and SP-4 *vs.* SP-2 (**B**, spectra **3** and **4**, respectively) with donor (*N,N*-dialkylaminonaphthalene or *N,N*-dimethylaminobenzyl) and acceptor (pyrene) partners swapped (see Table 1 for the structures). Spectra were recorded at 10 °C in 80% TFE–10mM Tris buffer, pH 8.4, 0.1 M NaCl with component concentrations of 2.5 μM (1 : 1 : 1); λ_{ext} 350 nm. Due to the very different fluorescence intensity of Pyr-5′-ON1 and ON2-3′-Pyr oligo probes, spectra were scaled against the pyrene LES band at 380 nm to compare *exciplex*:*LES* ratios for the systems studied.

split-probe systems possessing the same exci-partner (pyrene) at the 5′-terminal phosphate of the ON1 oligo probe and different exci-partners (pyrenyl, *N,N*′-dialkylaminonaphthaleno or dimethylaminobenzyl, respectively) at the 3′-terminal phosphate of the ON2 oligo probe (spectra are scaled against LES emission band of the pyrene at 380 nm as a reference to allow comparison of *exciplex*:*LES* or *excimer*:*LES* ratios (I_E/I_M) for these systems). It is seen that I_E/I_M is highest for SP-1, possessing pyrene as a second partner. The replacement of 3′-pyrene by 3′-*N,N*-dialkylaminonaphthalene (SP-19) resulted in a marked decrease in I_E/I_M. Further replacement of the 3′-partner group by 3′-*N,N*-dimethylaminobenzyl (SP-4) resulted in an additional decrease in the relative intensity of the exciplex band. A similar effect was observed when SP-2 and SP-18 (with the reversed location of donor and acceptor groups) were compared with the SP-1 system (Fig. 6B). Detailed evaluation of these types of structural effects requires time-resolved measurements, as indicated by a referee, and such studies are in progress.

(ii) Effect of *N*-alkylation of donor exci-partners. The electron-donating properties of an exci-partner strongly depend on the *nature* and *number* of *N*-alkyl substitution group(s) in the aminobenzyl or aminonaphthaleno aromatic groups. Comparison of SP-18 (with an *N,N*-dialkylaminonaphthalene group) and SP-20 (with an *N*-alkylaminonaphthaleno donor partner) showed that the relative integral intensity of the exciplex band is slightly higher
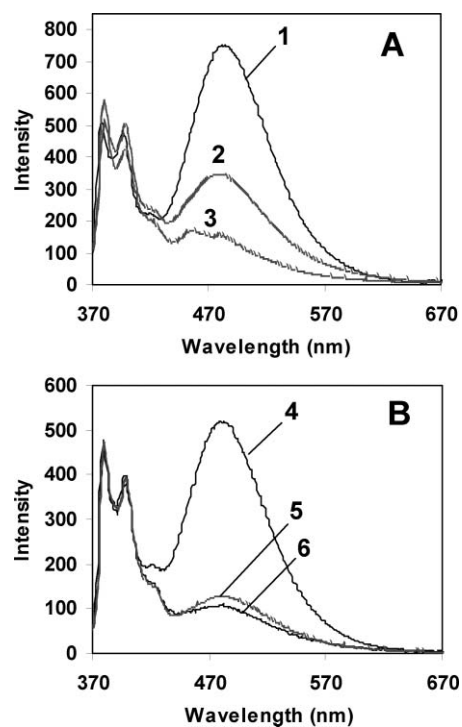
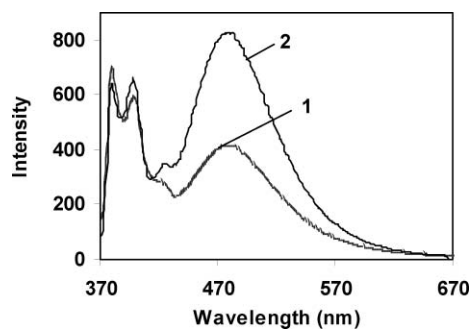**Fig. 6** **A**: Comparison of the emission spectra of systems SP-1, SP-19 and SP-4 with a fixed exci-partner (pyrene) at the 5′-terminal phosphate site of the ON1 oligo probe and different exci-partners (pyrenyl, *N,N*′-dialkylaminonaphthaleno or dimethylaminobenzyl, respectively) at the 3′-terminal phosphate site of the ON2 oligo probe. **1**: SP-1 excimer system containing two pyrenyl exci-partners; **2**: SP-19 exciplex system containing *N,N*-dimethylalkylaminonaphthaleno 3′-donor partner; **3** SP-4 exciplex system containing a dimethylaminobenzyl 3′-donor partner. **B**: Comparison of the emission spectra of systems SP-1, SP-18 and SP-2 with a fixed exci-partner (pyrene) at the 3′-terminal phosphate site of the ON2 oligo probe and different exci-partners (pyrenyl, *N,N*′-dialkylaminonaphthaleno or dimethylaminobenzyl, respectively) at the 5′-terminal phosphate site of the ON1 oligo probe. **4**: SP-1 excimer system containing two pyrenyl exci-partners; **5**: SP-18 exciplex system containing an *N,N*′-dialkylaminonaphthaleno 5′-donor partner; **6**: SP-2 exciplex system containing a dimethylaminobenzyl 5′-donor partner. Spectra were recorded at 10 °C in 80% TFE–10 mM Tris, pH 8.3, 0.1 M NaCl; λ_{ext} 350 nm.

for SP-18 than for SP-20, and the λ_{em} value for the *N*-methyl donor (485 nm) is at longer wavelength than that for the N–H variant (480 nm) of the naphthalene donor (data not shown).

(iii) Effect of linker structure. One way to improve the performance of DNA-mounted exciprobes is to design linker groups connecting donor and acceptor partners to the oligo probes that could prevent unfavourable interactions of hydrophobic exci-partners with DNA nucleotide bases and/or encourage interactions between exci-partners. Success in this strategy was demonstrated by SP-26, which is a structural analogue of the SP-19 system, but possesses an alternative linker group. In the SP-26 system the ethylenediamine linker connecting 5′-pyrene to the DNA was replaced by a negatively charged aspartate fragment to induce repulsion of the pyrene group from the DNA sugar–phosphate surface. Fig. 7 shows that the *exciplex*:*LES ratio* is significantly enhanced for the SP-26 system (spectrum 2) compared with the original SP-19 system (spectrum 1). However,

Fig. 7 Comparison of emission spectra of systems SP-19 and SP-26 possessing different linker groups. **1**: SP-19 system with an ethylenediamine linker connecting both exci-partners; **2**: SP-26 system with a negatively charged aspartate linker connecting the 5′-pyrenyl to ON1 oligo probe and ethylenediamine linker connecting the 3′-N,N'-dialkylaminonaphthaleno exci-partner to ON2 oligo probe. Spectra were recorded at 10 °C (without heating–re-cooling) cycle in 80% TFE–10 mM Tris, pH 8.3, 0.1 M NaCl; λ_{ext} 350 nm.

in pure aqueous solutions SP-26 did not produce an emissive exciplex.

Excimer system SP-25 (a structural analogue of SP-1) with two pyrenyl exci-partners attached to oligo probes *via* aspartate linkers showed good excimer emission in the presence of 80% TFE (see Table 2). However, in aqueous solutions SP-25 produced a fairly weak excimer band (data not shown), which was similar to that observed for SP-1 (Fig. 2) under identical conditions. For excimer systems SP-40 and SP-41 with 'mixed' linker groups (see Table 1 for structures), the *exciplex:LES* ratio (I_E/I_M) was rather low even in the presence of TFE (Table 2). A possible explanation could be that pyrenyl partner attached *via* a non-charged ethylenediamine linker may still be involved in competitive interactions with DNA, which discourage its interaction with the second partner and thus reduce excimer emission.
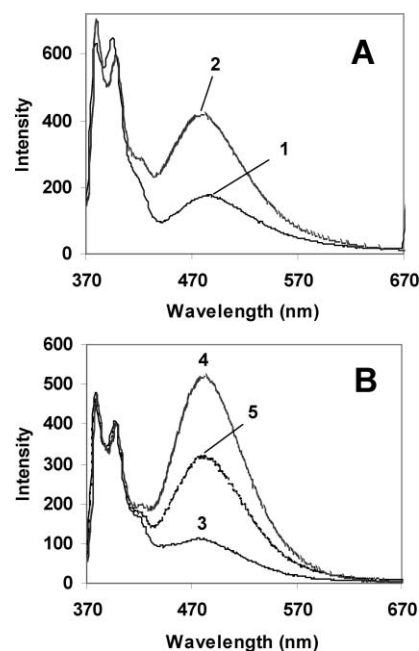
In an attempt to further improve excimer/exciplex emission, we designed system SP-27, SP-28 and SP-29 (see Table 1), which are structural analogues of systems SP-19, SP-18 and SP-1, respectively. Systems SP-27, SP-28 and SP-29 possess an

oligopeptide linker (-Ala(Gly)₄-) connecting both pyrenyl and N,N'-dialkylaminonaphthaleno exci-partners to the 5′- or 3′-terminal phosphate groups of the oligo probes. These have the potential for hydrogen bonding between the main chain carbonyl oxygen and amide groups of the peptide linkers, as in β-sheet structures in proteins.[29,30] This could bring the exci-partners close together, favouring efficient excimer/exciplex emission. The exci-partners were thus separated from the nucleotides by five amino acid residues. However, it was shown that SP-19, SP-18 and SP-1 systems, with the short ethylenediamine linker groups, produced much stronger exciplex emission than the corresponding peptide-based versions SP-27, SP-28 and SP-29, respectively. Fig. 8 gives examples of inferior emission of peptide systems SP-27 (curve 1) and SP-29 (curve 3) compared to their structural analogues SP-19 (curve 2) and SP-1 (curve 4), respectively (see the Discussion section). In small organic intramolecular systems, the efficiency of exciplex formation from exciplex partners linked by variable-length CH_2 chains depends on the chain length.[31,32] In such systems, rotational/conformational effects govern the relative location of the exciplex partners. However, in these new DNA constructs the situation is rather different. The present exciplex constructs on DNA are not directly comparable, as the exciplex partners are borne on the tips of two chains (in the context of this

Table 2 Fluorescence emission data collected at 10 °C and melting temperature values obtained for exciplex and excimer systems in 80% TFE/10 mM Tris, pH 8.3, 0.1 M NaCl; λ_{ext} 350 nm except where indicated[a]

System	λ_{em}/nm	I_E/I_M	T_m measured at λ_{em}^{max}
SP-1	486	1.18	27.0 ± 0.5
SP-25	487	0.83	26.0 ± 0.5
SP-2	484	0.22	25.0 ± 1.0
SP-4	480	0.28	26.0 ± 1.0
SP-3	480	0.19	N/D
SP-18	485	0.27	26.0 ± 1.0
SP-19	482	0.61	26.0 ± 1.0 [b]
SP-20	480	0.21	N/D
SP-26	484	1.18	N/D
SP-40	481	0.57	25.0 ± 0.5
SP-41	481	0.23	25.0 ± 0.5 [c]
SP-27	484	0.45	N/D
SP-28	483	0.48	N/D
SP-29	484	0.23	N/D

[a] N/D: not determined. [b] T_m based on A_{260} was 25.0 °C (ref. 12). [c] The melting temperature measured at λ_{em} 376 nm for the LES of pyrene was 25.0 ± 0.5 °C.

Fig. 8 Effect of an oligopeptide linker (-Ala(Gly)₄-) on the performance of exciprobes. **A**: Emission spectrum of the exciplex-based system SP-27 (**1**) with oligopeptide linker (-Ala(Gly)₄-) connecting both pyrenyl and N,N'-dialkylaminonaphthaleno exci-partners to the 5′- and 3′-terminal phosphates of the oligo probes, respectively, *versus* its structural analogue SP-19 (**2**), containing short ethylenediamine linker groups. **B**: Emission spectrum of excimer-based system SP-29 (**3**) with oligopeptide linker (-Ala(Gly)₄-) connecting two pyrenyl exci-partners to the 5′- and 3′-terminal phosphate groups of the oligo probes *versus* the structural analogue SP-1 (**4**), containing short ethylenediamine linker groups. Spectrum (**5**) is the emission spectrum of the re-annealed SP-29 system following a heating–re-cooling cycle. Spectra were recorded at 10 °C in 80% TFE–10 mM Tris, pH 8.3, 0.1 M NaCl; λ_{ext} 350 nm.

particular paragraph it is peptides, but not for all the structures we describe) that are connected though a duplex of DNA chains held by a consortium of hydrogen bonds and stacking interactions.

For excimer system SP-29, containing two pyrenyl exci-partners attached to oligo probes *via* the peptide linker, it was possible to improve exciplex emission by a heating–re-cooling cycle (curve 5).

Melting profiles

Melting temperature profiles were obtained for the studied split-probe systems (Table 1) by monitoring fluorescence emission intensity as function of temperature increase (from 5 °C to 60 °C) following detection at both exciplex λ_{em} (480 nm) and LES λ_{em} (376 nm). Fig. 9 shows melting temperature profiles for the SP-41 system as a typical example of such thermal denaturation. The sigmoidal temperature dependence of the exciplex emission signal disappearance (monitored at 480 nm; curve 1) and of the LES emission band re-appearance (monitored at 376 nm; curve 2) corresponds to a DNA duplex melting profile typical of the dsDNA to ssDNA transition. These data provide further evidence of tandem duplex formation, showing only one transition, consistent with literature findings that duplex structures containing a backbone nick in one of the strands melt cooperatively.[33–35] T_m values, along with summarised data for fluorescence emission maxima and I_E/I_M values, are collected in Table 2.
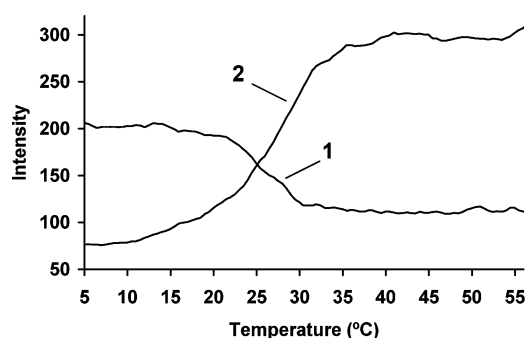
Fig. 9 Melting curves for the excimer system SP-41 (ON1-5′-AspPyr + ON2-3′-Pyr + Target), plotting relative fluorescence emission at 480 nm (**1**, λ_{ext} 350 nm) and at 376 nm (**2**, λ_{ext}, 340 nm) against temperature in 80% TFE/Tris buffer (10 mM Tris, 0.1 M NaCl, pH 8.3); component concentration 2.5 µM.

Discussion

Split-probe approach for exciplex-based detection of nucleic acids

In the last year two approaches using DNA-mounted exciplexes have been reported for detection of nucleic acids. In addition to our preliminary communication of the approach in the present study there is a report by Kashida *et al.* who demonstrated efficient exciplex emission in pure aqueous solution for the system with exciplex partners introduced into the middle of DNA.[14] In one specific example, exciplex partners (pyrene and *N*,*N*-dimethylaniline moieties) were located *face-to-face* in the DNA duplex. However, this approach requires both the oligo-probe and the target sequence to be labelled by exciplex chromophores, which may rather complicate bioassay conditions. Strong exciplex emission was also observed when both exciplex partners were consecutively positioned in the middle of the single DNA oligo

probe. However, in the case of successive location of exciplex partners, even a single-stranded oligo-probe produced exciplex emission, giving an undesirable background signal. For detection of single-base insertions and deletions, the exciplex partners were separated by one nucleotide residue to block interaction between them and thus prevent exciplex emission on hybridization with perfect match. Hybridisation with the target containing a single-base deletion resulted in looping of the unhybridised probe region containing exciplex partners, which induced interaction between the two exciplex chromophores accompanied by exciplex emission. Although this research clearly demonstrates that exciplex emission can be observed even in aqueous solution, the disadvantage of this method was a prerequisite of secondary structure formation on hybridization (*e.g.* looping of the fragment possessing exciplex partners). Also, although this method succeeded in detection of insertions and deletions, the application of this approach to the DNA mismatch detection has not yet been reported for it.

The alternative split-probe approach of the present study uses externally oriented DNA-mounted exciplexes, from two separate exciprobes designed to produce exciplex emission by being specifically assembled *in situ* by hybridisation with a bio-target. In this case, a unique fluorescence signal can be generated *only* after specific self-assembly of signal-silent exciplex components with a perfectly matched target. The advantage of the exciplex-based split-probe approach is low or zero background, ultra-biospecificity, and ability to detect DNA mismatches.

Melting temperature studies

T_m profiles for split-probe systems (Table 1) were obtained by monitoring fluorescence intensity from 5 to 60 °C for both exciplex/excimer λ_{em} (480 nm) and LES λ_{em} (376 nm). Melting curves presented in Fig. 9 for the excimer system SP-41 provide a pictorial example of thermal denaturation of such split-probe systems in the presence of 80% TFE. Melting profiles reflect thermal denaturation of the duplex, causing the dissociation of the 8-mer split-probes from the duplex, which results in separation of exci-partners. This is accompanied by eventual disappearance of exciplex/excimer signal and subsequent re-appearance of the LES fluorescence band, previously quenched within the excited state complex. The sigmoidal nature of the melting curves, typical of the transition of dsDNA to ssDNA, provides evidence that presence of co-solvent (80% TFE) does not disrupt duplex formation. However, T_m values in the presence of 80% TFE were typically 10–11 °C lower than in purely aqueous solutions, demonstrating the destabilisation effect of the TFE co-solvent, presumably attributable to a decrease of hydrophobic stacking interactions of nucleotide bases, or a change in duplex structure. T_m values calculated from the melting profiles (Table 2) were very similar for all split-probe systems studied, ranging between 25.0 ± 0.5 and 27.0 ± 0.5 °C, reflecting similarity in the duplex stabilities for these systems. SP-1 was the most stable (T_m = 27.0 ± 0.5 °C), presumably due to the presence of two pyrenyl residues, which are known to stabilise DNA duplexes.[33,34]

TFE co-solvent for exciplex/excimer signal development

In model organic systems corresponding to the SP-19 and SP-4 cases, solvent polarity was found to have very little effect on the

emission wavelength (λ_{em}) of the LES of the pyrenyl partner. In contrast, exciplex emission showed a much greater dependence on solvent dielectric constant, with λ_{em} varying over a range of nearly 100 nm on going from cyclohexane (ε 2.0) to *N*-methylformamide (ε 182).[11] This is consistent with the extensive literature showing that solvent polarity is crucial to the properties of exciplexes.[10] However, exciplex emission is more than just a matter of solvent polarity in these DNA-mounted exciplex cases because out of the many solvents tested only a few were able to induce exciplex emission and of these, TFE was especially favourable. Exciplex emission was not observed for various co-solvents (50 and 70% v/v tested), *viz.* methanol, ethanol, acetone, hexafluoropropan-2-ol or tetrafluoropropan-1-ol. Exciplex emission for the fully assembled system was strongly and specifically enhanced by trifluoroethanol (TFE), and weakly by ethylene glycol and ethylene glycol dimethyl ether ($\sim$5 and 10-fold less than TFE, respectively).[13] The origins of the rather specific effects of TFE on exciplex emission for DNA systems is difficult at this stage to explain unambiguously and probably arises from a combination of factors. TFE has a particular ability to induce a structural transition in DNA favouring a shift from B-like to A-like.[36] However, by changing the hydrophobicity of the environment, this co-solvent also regulates the excited-state attraction of the exci-partners through (i) affecting their relative attraction for each other in the excited state (and perhaps also in the ground state) and (ii) through the long-established stronger exciplex emission in lowered polarity environments.[9,37–39]

Hydrophobic interactions between donor and acceptor in model intramolecular organic exciplexes with the same types of donor and acceptor pairs as in the present study stabilise a pre-formed stacking structure detected by cross-peaks between them in NOESY NMR experiments.[11] In polar media, such as for the DNA systems of the present study, this would enhance the probability of the exci-partners forming their excited-state complex on photo-excitation. Our observations show that hydrophobic properties of the exci-partners significantly enhance exciplex emission (see next section). However, aromatic nucleotide bases may competitively interact with exci-partners *via* formation of non-specific hydrophobic contacts with donor or/and acceptor partners thus preventing exciplex formation. Our NMR and UV-visible data[33,34] provide strong evidence of strong hydrophobic interactions of a pyrenyl group with the DNA part of a split-probe. This competition would act to discourage favourable interactions between exci-partners, especially if one of them is not hydrophobic enough to compete with pyrene–DNA interactions. Therefore, the exci-partners should possess similar hydrophobic properties to increase the chance of exciplex/excimer formation. The use of specific co-solvents has also been noted in other systems that operate by the principles of Fig. 1. Thus, Masuko *et al.* studied an excimer-based split-probe system using DMF as a hybridisation co-solvent, in analogy to the use of formamide to weaken base-pairing, and found that an optimal amount was 20% v/v.[5] The DMF was also proposed to influence fluorescence quantum yields through an effect on pyrene–solvent dipole–dipole interactions.[5]

Hydrophobic and electron donor/acceptor properties of the exci-partners. Our studies of DNA-mounted exciplex/excimer split-probe systems show that a reasonable compromise in hydrophobic properties of exci-partners has to be achieved for successful exciplex/excimer formation. The excimer system SP-1 possessing two pyrenyl exci-partners produced the strongest signal at 480 nm (both in absolute terms and, as shown in Fig. 6, when normalised to the LES of pyrene) in comparison with SP-19, SP-18, SP-4 and SP-2 exciplex systems with the second exci-partner replaced by *N*,*N*-dimethylaminonaphthalenyl or *N*,*N*-dimethylaminophenyl. However, it is hard to directly compare excimers and exciplexes in view of the different degrees of charge transfer involved in their emissive excited states. Formation of excited-state complexes also depends on the ionisation potentials of the partners.

Effect of linker group on exciplex formation. The linkers connecting the exci-partners to the oligo-probes strongly affect the ability of donor and acceptor to interact and thus play an important role in excimer/exciplex formation. Our studies demonstrate that correctly designed linker groups significantly enhance exciplex formation. Replacement of the neutral ethylenediamine linker with a negatively charged aspartate fragment (*e.g.* system SP-26) notably enhanced exciplex emission, presumably due to the induced repulsion of the pyrene group from the negatively charged sugar–phosphate surface of DNA (Fig. 8). Excimer system SP-25 with aspartate linker groups connecting both pyrene partners to the oligo probes showed detectable excimer emission even in pure aqueous solutions, similar to that observed for SP-1 (Fig. 2).

Another attempt in improving exciplex formation was based on use of peptide fragments as linker groups to induce chain interactions between the two linkers, thereby bringing the exci-partners close and stabilising their interactions. This should have resulted in an increase in excimer/exciplex emission relative to the short linker systems. However, exciplex emission of peptide-based systems was lower than the short-linker analogues. It is therefore possible that no defined structure formed between the two peptide linker systems. β-Sheet formation in proteins and peptides occurs intramolecularly through formation of a β-hairpin.[40] However, the peptide linkers in this study are separate molecules, and therefore may not form a β-sheet, especially in TFE media. While the junction of the split oligos could serve the role of the hairpin, it will be necessary to replace the conformationally unrestrained glycine residues, which are known to destroy secondary structure.[29] Although interaction of the exci-partners did occur within peptide-based systems SP-27, SP-28 and SP-29, exciplex emission between exci-partners was reduced, presumably due to the high conformational flexibility of these long linker groups reducing the probability of collisions between exci-partners.

Conclusions

This research has investigated contributions from various factors on exciplex performance within DNA tandem systems. These factors include the relative hydrophobicities of the partners used in the exciprobes, the medium in which the systems are studied, the electron-donating and electron-accepting characteristics of the exci-partners, and the structures and charge distributions of linker groups. Careful design of exci-partners and linker groups, as well as appropriate experimental design (*e.g.* media, use of a heating–re-cooling cycle, *etc.*) significantly enhances exciplex/excimer emission signal for DNA-mounted exciplexes.

This journal is © The Royal Society of Chemistry 2007

Org. Biomol. Chem., 2007, **5**, 1039–1051 | 1047

Methods

Pyren-1-ylmethylamine hydrochloride, (4-(aminomethyl)phenyl)-dimethylamine hydrochloride, *N*-(naphthalen-1-yl)ethane-1,2-diamine dihydrochloride and (4-(dimethylamino)phenyl)acetic acid for the preparation of ON1-5′-Pyr, ON2-3′-Pyr, ON1-5′-DMA, ON2-3′-DMA, ON1-5′-NHNp, ON2-3′-NHNp and ON1-5′-C7DMA, respectively, were purchased from Sigma-Aldrich Chemical Co., (Poole, Dorset, UK). *N*-Methyl-*N*-(naphthalen-1-yl)ethane-1,2-diamine dihydrochloride for the preparation of ON1-5′-NmeNp and ON2-3′-NmeNp oligo probes was synthesised as described.[13] Oligodeoxynucleotides were purchased from Eurogentec (Liege, Belgium) and Sigma-Aldrich-Proligo (Paris, France). Cetyltrimethylammonium bromide, triphenylphosphine, dipyridyldiphosphate, dimethylaminopyridine, triethylamine, lithium perchlorate, dimethylformamide, hydroxybenzotriazole, *N*-methylmorpholine and dicyclohexylcarbodiimide were purchased from Sigma-Aldrich Chemical Co., (Poole, Dorset, UK). H-BocAla(Gly)$_4$-OH was purchased from Bachem (St Helens, UK).

Attachment of H-BocAla(Gly)$_4$-OH peptide linker to pyren-1-ylmethylamine and *N*-methyl-*N*-(naphthalen-1-yl)ethane-1,2-diamine

H-BocAla(Gly)$_4$-OH was attached to pyren-1-ylmethylamine and *N*-methyl-*N*-(naphthalen-1-yl)ethane-1,2-diamine according to Scheme 1 for subsequent preparation of ON1-5′-Pept-Pyr, ON2-3′-Pept-Pyr, ON1-5′-Pept-NMeNp and ON3-3′-Pept-NMeNp oligo probes.

Pyren-1-ylmethylamine hydrochloride (**VI**) (0.25 g, 0.82 mmol) or *N*-methyl-*N*-(naphthalen-1-yl)ethane-1,2-diamine (**VII**) (0.20 g, 0.82 mmol) and triethylamine (0.11 ml, 0.82 mmol) were dissolved in DMF (15 mL) and stirred at room temperature for 30 min. H-BocAla(Gly)$_4$-OH (0.25 g, 0.82 mmol), hydroxybenzotriazole (0.11 g, 0.82 mmol) and *N*-methylmorpholine (0.091 mL, 0.82 mmol) were then added, the reaction mixture cooled in an ice bath and dicyclohexylcarbodiimide (0.18 g, 0.86 mmol) added. The reaction mixture was stirred in the ice bath for 1 h, then refluxed for several hours, and stirred at room temperature overnight. The mixture was filtered to remove the urea formed, and DMF removed *in vacuo*. The residue was dissolved in ethyl acetate (50 mL) and extracted with 25 mL portions of saturated sodium hydrogen carbonate, 10% citric acid, sodium hydrogen carbonate

and finally water. The organic layer was dried over anhydrous sodium sulfate and the solvent removed *in vacuo* to give the crude product **IX** or **X** as an orange solid (see Scheme 1).

To remove the Boc protecting group, a solution of **IX** or **X** in 50% TFA and 2% triethylsilane in methanol (total volume 20 mL) was stirred for several hours at room temperature until TLC (ethyl acetate–methanol 60 : 40) showed complete reaction. Solvents and by-products were removed *in vacuo* and the product **XI** or **XII** recrystallised from hexane and methanol as a slightly orange solid, which was characterised by ^{1}H NMR spectroscopy.

^{1}H NMR of **XI** (MeOD): δ_H 1.46 (d, 3H, CH$_3$, Ala), 3.87–3.96 (m, 8H, 4 × CH$_2$, Gly), 4.01–4.12 (m, 1H, CH, Ala), 5.14 (s, 2H, -CH$_2$NH- of pyrenemethylamino group), 8.00–8.36 (m, 9H, 9 × Ar-H, pyrene).

^{1}H NMR of **XII** (D$_2$O): δ_H 1.41 (d, 3H, CH$_3$ of Ala), 2.86 (s, 3H, -NCH$_3$), 3.43 (m, 2H, -CH$_2$NHCO-), 3.61 (m, 2H, -CH$_2$NMe-), 3.87–3.82 (m, 8H, 4 × CH$_2$, Gly), 4.01–4.12 (m, 1H, CH, Ala), 7.22–8.32 (m, 7H, 7 × ArH, naphthyl).

Conjugation of exci-partners to oligonucleotide probes ON1 and ON2

In general, attachment of exci-partners bearing an aliphatic amine functional group to the 5′- or 3′-terminal phosphate group of oligonucleotide probes ON1 and ON2 followed by purification and characterisation was achieved according to the published protocols.[13] β-(Pyren-1ylmethylaminocarboxamide)aspartic acid (a gift from Dr Ben Law and AnMat Co., Manchester) was attached similarly through its α-amino group, to give ON1-5′-AspPyr and ON2-3′-AspPyr. ON1-5′-Pyr and ON2-3′-NMeNp oligo probes were characterised as described elsewhere.[13]

ON1-5′-NMeNp: ^{1}H NMR (D$_2$O): δ_H 1.77–1.86 (s, 12H, 4 × CH$_3$, 4 × dT), 2.15–2.92 (m, 16H, 8 × H2′ and 8 × H2″ sugar ring protons), 2.79 (s, 3H, NCH$_3$), 3.22 (t, 2H, -NHCH$_2$-), 3.43 (t, 2H, -NHCH$_2$-), 3.60–4.60 (m, 24H, 8 × H4′, 8 × H5′ and 8 × H5″ sugar ring protons), 5.4–6.40 (m, 8H, 8 × H1′ of sugar ring and d, 1H, H5 of dC), 7.16–8.14 (m, 7H, 7 × Ar-H, naphthyl, s, 7H, 7 × Ar-H from each dG (×3) and dT (×4); d, 1H, H6 of dC). The H3′ sugar ring proton region (4.90–5.20 ppm) was not analysed due to suppression of residual water signal at 4.8 ppm. The UV-visible absorption spectra of ON1-5′-NMeNp showed a shoulder at 310 nm on the 260 nm absorption band, indicating the presence of naphthalene.
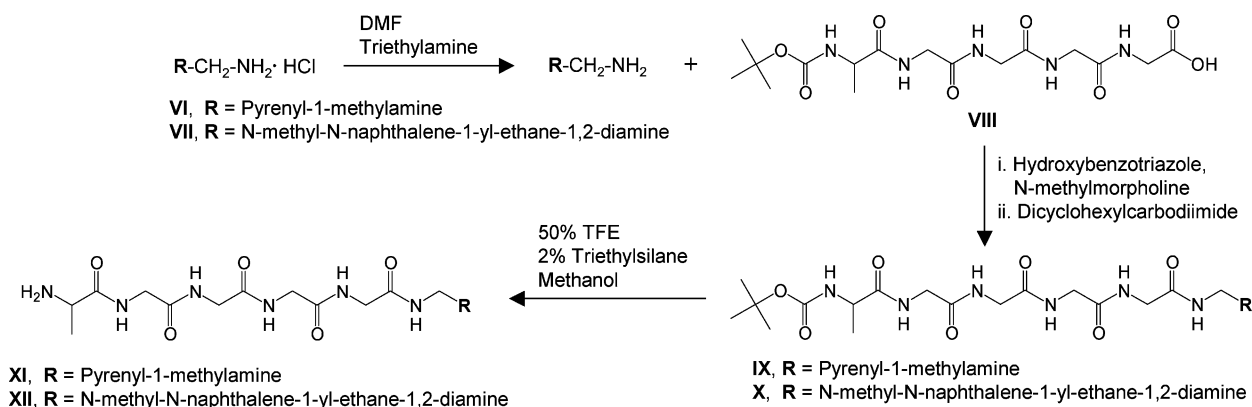
Scheme 1 Attachment of H-BocAla(Gly)$_4$-OH peptide linker to pyren-1-ylmethylamine and *N*-methyl-*N*-(naphthalen-1-yl)ethane-1,2-diamine.

ON2-3′-Pyr: ^{1}H NMR (D$_2$O): δ_H 1.66–1.70 (s, 9H, 3 × CH$_3$ of 3 × dT), 2.13–2.93 (m, 16H, 8 × H2′ and 8 × H2″ sugar ring protons), 3.60–4.60 (m, 24H, 8 × H4′, 8 × H5′, 8 × H5″ sugar ring protons; bs, 2H, -NHCH$_2$-), 5.4–6.40 (m, 8H, 8 × H1′ of sugar; d, 2H, 2 × H5 of 2 × dC), 6.91–8.34 (m, 9H, 9 × Ar-H of pyrene; s, 7H, 7 × Ar-H from nucleotide bases (1 from each dG (×2) and dT (×3), 2 from dA); d, 2H, H6 of dC (×2)). The resonance area of H3′ sugar ring protons (4.90–5.20 ppm) was not analysed due to suppression of residual water signal at 4.8 ppm. The presence of pyrene alters the UV-visible absorption spectrum of ON2-3′-Pyr, leading to an additional band around 345 nm, and altering the band at 260 nm. The ratio between the absorbances at 260 and 345 nm was around 3.0, typical of mono-pyrene-substituted 8-mer oligonucleotides.

ON1-5′-DMA: ^{1}H NMR (D$_2$O): δ_H 1.76–1.87 (s, 12H, 4 × CH$_3$ of 4 × dT), 2.15–2.92 (m, 16H, 8 × H2′ and 8 × H2″ sugar ring protons), 2.60–2.63 (d, 6H, -N(CH$_3$)$_2$), 3.60–4.60 (m, 24H, 8 × H4′, 8 × H5′, 8 × H5″ sugar ring protons; bs, 2H, -NHCH$_2$-), 5.4–6.40 (m, 8H, 8 × H1′ of sugar ring; d, 1H, H5 of dC), 7.16–8.14 (s, 7 × Ar-H from each dG (×3) and dT (×4); d, 1H, H6 of dC) 6.62–7.02 (d, 4H, 4 × Ar-H of N,N-dimethylaminobenzyl). The H3′ sugar ring proton region (4.90–5.20 ppm) was not analysed due to suppression of residual water signal at 4.8 ppm.

ON2-3′-DMA: ^{1}H NMR (D$_2$O): δ_H 1.65–1.71 (s, 9H, 3 × CH$_3$ of 3 × dT), 2.15–2.92 (m, 16H, 8 × H2′ and 8 × H2″ sugar ring protons), 2.60–2.63 (d, 6H, -N(CH$_3$)$_2$); 3.60–4.60 (m, 24H: 8 × H4′, 8 × H5′, 8 × H2″ sugar ring protons; bs, 2H, -NHCH$_2$); 5.4–6.40 (m, 8H, 8 × H1′ of sugar ring; d, 2H, 2 × H5 of 2 × dC), 6.62–7.02 (d, 4H, 4 Ar-H of N,N-dimethylaminobenzyl), 6.91–8.34 (s, 7H, Ar-H from nucleotide bases (1 from each dG (×2), and dT (×3), 2 from dA); d, 2H, H6 of dC (×2)). The resonance region of H3′ sugar ring protons (4.90–5.20 ppm) was not analysed due to suppression of residual water signal at 4.8 ppm.

ON1-5′-Pept-Pyr: ^{1}H NMR (D$_2$O): δ_H 1.00–1.03 (d, 3H, CH$_3$ of alanine), 1.50–1.64 (s, 12H, 4 × CH$_3$ of 4 × dTs), 2.15–2.92 (m, 16H, 8 × H2′ and 8 × H2″ sugar ring protons), 3.87–3.96 (m, 8H, 4 × CH$_2$ of 4 Gly residues), 3.60–4.60 (m, 32H, 8 × H4′, 8 × H5′, 8 × H5″ sugar ring protons, 4 × CH$_2$ of 4 Gly residues; bs, 2H, -NHCH$_2$-), 5.4–6.40 (m, 8H, 8 × H1′ of sugar ring; d, 1H, H5 of dC), 6.60–8.16 (m, 9H, 9 × Ar-H from pyrene; s, 7H, 7 × Ar-H from each dG (×3) and dT (×4); d, 1H, H6 of dC). The H3′ sugar ring proton region (4.90–5.20 ppm) was not analysed due to suppression of residual water signal at 4.8 ppm. The presence of pyrene alters the UV-visible absorption spectrum of ON1-5′-Pept-Pyr, leading to an additional band around 345 nm, and altering the band at 260 nm. The ratio between the absorbances at 260 and 345 nm was around 3.0, typical of mono-pyrene-substituted 8-mer oligonucleotides.

ON2-3′-Pept-Pyr: ^{1}H NMR (D$_2$O): δ_H 1.35–1.38 (d, 3H, CH$_3$ of Ala), 1.65–1.66 (s, 9H, 3 × CH$_3$ of 3 × dT), 2.15–2.92 (m, 16H, 8 × H2′ and 8 × H2″ sugar ring protons), 3.60–4.60 (m, 32H, 8 × H4′, 8 × H5′, 8 × H5″ sugar ring protons, 4 × CH$_2$ of 4 Gly residues; d, 2H, -NCH$_2$); 5.4–6.40 (m, 8H, 8 × H1′ of sugar ring; d, 2H, 2 × H5 of 2 × dC), 6.91–8.34 (m, 9H, 9 × Ar-H from pyrene; s, 7H, 7 × Ar-H from nucleotide bases (1 from each dG (×2) and dT (×3), 2 from dA); d, 2H, H6 of dC (×2)). The H3′ sugar ring proton region (4.90–5.20 ppm) was not analysed due to suppression of the residual water signal at 4.8 ppm. The presence of pyrene alters the UV-visible absorption spectrum of ON2-3′-Pept-Pyr, leading to an

additional band around 345 nm, and altering the band at 260 nm. The ratio between the absorbances at 260 and 345 nm was around 3.0, typical of mono-pyrene-substituted 8-mer oligonucleotides.

ON1-5′-Pept-NMeNp: ^{1}H NMR (D$_2$O): δ_H 1.00–1.03 (d, 3H, CH$_3$ of Ala);1.54–1.64 (s, 12H, 4 × CH$_3$ of 4 × dT), 2.15–2.92 (m, 16H, 8 × H2′ and 8 × H2″ sugar ring protons), 2.60 (s, 3H, N-CH$_3$), 3.22 (t, 2H, -NHCH$_2$-), 3.43 (t, 2H, -NHCH$_2$-), 3.60–4.60 (m, 32H, 8 × H4′, 8 × H5′, 8 × H5″ sugar ring protons and 4 × CH$_2$ of 4 Gly residues), 5.4–6.40 (m, 8H, 8 × H1′ of sugar ring; d, 1H, H5 of dC), 6.92–8.14 (m, 7H, 7 × Ar–H, naphthyl; s, 7H, 7 × Ar-H from each dG (×3) and dT (×4); d, 1H, H6 of dC). The H3′ sugar ring proton region (4.90–5.20 ppm) was not analysed due to suppression of residual water signal at 4.8 ppm. The UV-visible absorption spectra of ON1-5′-Pept-NMeNp showed a shoulder at 310 nm on the 260 nm absorption band, indicating the presence of naphthalene.

ON2-3′-Pept-NMeNp: 1H NMR (δH, D$_2$O): δ_H 1.35–1.38 (d, 3H, CH$_3$ of Ala), 1.42–1.64 (s, 9H, 3 × CH$_3$ of 3 × dT), 2.15–2.92 (m, 16H, 8 × H2′ and 8 × H2″ sugar ring protons), 2.67 (s, 3H, N-CH$_3$), 3.22 (t, 2H, -NHCH$_2$-), 3.43 (t, 2H, -NHCH$_2$-), 3.60–4.60 (m, 32H, 8 × H4′, 8 × H5′, 8 × H5″ sugar ring protons; 4 × CH$_2$ of 4 Gly residues); 5.4–6.40 (m, 8H, 8 × H1′ of sugar; d, 2H, 2 × H5 of 2 × dC), 6.91–8.34 (m, 7H, 7 × Ar-H of N′-methyl-N′-naphthyl; s, 7H, 7 × Ar-H from nucleotide bases (1 from each dG (×2) and dT (×3), 2 from dA); d, 2H, H6 × 2 of dC (×2)). The resonance area of H3′ sugar ring protons (4.90–5.20 ppm) was not analysed due to suppression of residual water signal at 4.8 ppm. The UV-visible absorption spectra of ON2-3′-Pept-NmeNp showed a shoulder at 310 nm on the 260 nm absorption band, indicating the presence of naphthalene.

ON1-5′-NHNp: ^{1}H NMR (D$_2$O): δ_H 1.77–1.86 (s, 12H, 4 × CH$_3$, 4 × dT), 2.15–2.92 (m, 16H, 8 × H2′ and 8 × H2″ sugar ring protons), 3.22 (t, 2H, -NHCH$_2$-), 3.43 (t, 2H, -NHCH$_2$-), 3.60–4.60 (m, 24H, 8 × H4′, 8 × H5′ and 8 × H5″ sugar ring protons), 5.4–6.40 (m, 8H, 8 × H1′ of sugar ring; d, 1H, H5 of dC), 7.16–8.14 (m, 7H, 7 × Ar-H, naphthyl; s, 7H, 7 × Ar-H from each dG (×3) and dT (×4); d, 1H, H6 of dC). The H3′ sugar ring proton region (4.90–5.20 ppm) was not analysed due to suppression of residual water signal at 4.8 ppm. The UV-visible absorption spectra of ON1-5′-NHNp showed a shoulder at 310 nm on the 260 nm absorption band, indicating the presence of naphthalene.

Preparation of ON1-5′-C7DMA oligonucleotide probe

Synthesis of the ON1-5′-C7DMA oligonucleotide probe containing the heptane-1,7-diamine linker (C-7) was achieved using two-step conjugation, $viz.$, initial coupling of heptane-1,7-diamine to the oligonucleotide followed by attachment of (4-(dimethylamino)phenyl)acetic acid to the free aliphatic amino group of the linker. Oligonucleotide ON1 (0.5 µmol, 35 ou$_{260}$) was dissolved in H$_2$O (100 µL) and precipitated by addition of 4% aqueous cetyltrimethylammonium bromide (20 µL). The sample was then centrifuged (5 min, 10 000 rpm) and the procedure repeated until there was no apparent precipitation after the addition of the cetyltrimethylammonium bromide. The supernatant was carefully removed and the pellet washed by water and dried under vacuum overnight.

A solution of oligonucleotide as the cetyltrimethylammonium salt in DMF (~150 µL) was treated with 2,2′-dipyridyl disulfide

(6.6 mg, 30 µmol) and triphenylphosphine (8 mg, 30 µmol) for 10 min, followed by treatment by 4-dimethylaminopyridine (6 mg, 50 µmol) for 10 min at 25 °C. The activated oligonucleotide was then precipitated using 2% LiClO$_4$ in acetone (2 mL), and the dried pellet dissolved in 1 M aqueous heptane-1,7-diamine (150 µL) and left for 1 h. On completion of reaction the oligonucleotide material was precipitated using 2% LiClO$_4$ in acetone (2 mL), dissolved in H$_2$O (100 µL) and purified by reverse-phase HPLC. The cetyltrimethylammonium salt of the oligonucleotide with the attached heptanediamine linker was prepared as described above and dissolved in anhydrous DMF (100 µL).

To a solution of (4-(dimethylamino)phenyl)acetic acid (17.9 mg, 100 µmol) in anhydrous DMF (100 µL), BOP (88.5 mg, 200 µmol) and 4-(dimethylamino)pyridine (24.4 mg, 200 µmol) were added and the mixture left for 30 min at 50 °C. The solution of oligonucleotide with attached heptanediamine linker was added and the resulting mixture left to react at 50 °C for 1 h. The reaction mixture was precipitated by addition of 2% LiClO$_4$ in acetone (2 mL), the supernatant discarded, the pellet dried, dissolved in H$_2$O (100 µL) and purified by reverse-phase HPLC.

ON1-5′-C7DMA: ^{1}H NMR (D$_2$O): δ_H 1.29–1.56 (m, 10H, 5 × -CH$_2$-) 1.76–1.87 (s, 12H, 4 × CH$_3$ of 4 × dT), 2.15–2.92 (m, 18H, 8 × H2′ and 8 × H2″ sugar ring protons; 2H, -CH$_2$NH-), 2.60–2.63 (d, 6H, -N(CH$_3$)$_2$), 3.21 (t, 2H, -CH$_2$NHCO-), 3.44 (s, 2H, -CH$_2$CO-) 3.60–4.60 (m, 24H, 8 × H4′, 8 × H5′, 8 × H5″ sugar ring protons); 5.4–6.40 (m, 8H, 8 × H1′ of sugar ring; d, 1H, H5 of dC), 6.62–7.02 (d, 4H, 4 Ar-H of N,N-dimethylaminobenzyl), 7.16–8.14 (s, 7 × Ar-H from each dG (×3) and dT (×4); d,1H, H6 of dC). The H3′ sugar ring proton region (4.90–5.20 ppm) was not analysed due to suppression of residual water signal at 4.8 ppm.

HPLC

Reverse-phase HPLC purification of oligonucleotides was performed using an HPLC Holochrome 302 (Gilson) chromatograph equipped with a C18 column (Vydac™, particle size 10 µm, inner diameter 10 mm, length 250 mm, pore size 300 Å) with elution using an increasing gradient (0–50%) of acetonitrile in water (fraction detection at 260 nm). In some cases HPLC purifications of probes were performed on an Agilent 1100 Series HPLC system, consisting of a quaternary pump with solvent degasser, a diode-array module for multi-wavelength signal detection using an Agilent 1100 Series UV-visible detector and an Agilent 1100 Series fluorescence detector for on-line acquisition of excitation/emission spectra. The system had a manual injector and thermostatted column compartment with two heat exchangers for solvent pre-heating. The HPLC system was operated through Agilent HPLC 2D ChemStation Software. Depending on the purification performed, the columns used were: Zorbax Eclipse X DB-C8 column (length 25 cm, inner diameter 4.6 mm, particle size 5 µm), or a Luna C18 (2) column (length 25 cm, inner diameter 4.6 mm, particle size 5 µm) with elution using an increasing gradient (0–50%) of acetonitrile in water (detection at 260, 280, and 340 nm).

Fluorescence spectroscopy

UV-Visible absorption spectra were measured at 20 °C on a Cary-Varian 1E UV-Visible spectrophotometer with a Peltier-thermostatted cuvette holder and Cary 1E operating system/2 (version 3) and the Cary 1 software. Quantification of the oligonucleotide components used millimolar extinction coefficients (ε_{260}) of 70.2 for ON1, 79.7 for ON2 and 169.4 mM^{-1} cm^{-1} for the 16-mer target. For the oligonucleotide probes ON1-5′-Pyr and ON2-3′-Pyr millimolar extinction coefficients (ε_{260}) were corrected taking into account millimolar extinction coefficients of pyren-1-ylmethylamine at 260 nm (ε_{260} for pyren-1-ylmethylamine in water was determined to be 15.34 mM^{-1} cm^{-1}). Fluorescence excitation and emission spectra were recorded on a thermostatted Shimadzu RF-5301 spectrofluorophotometer, or a Varian Eclipse Fluorescence Spectrophotometer with a Peltier-thermostatted cuvette holder. For comparative purposes the standard component concentration of tested samples in the cuvette was 2.5 µM. Spectra were recorded in Tris buffer (10 mM Tris, 0.1 M NaCl, at pH 8.5) containing various percentages of TFE or other co-solvents (0–80%) using a 2 mL or 100 µL thermostatted 4-sided quartz cuvette. Excitation wavelengths for both monomer and exciplex/excimer emission were optimised in each experiment and ranged from 340 to 350 nm. In most cases slitwidths were set from 5 to 10 nm both for excitation and emission spectra, depending on the intensity of emission. "Automatic shutter-on" regime was used to minimise photodegradation of compounds in the cuvette. All spectra were corrected for buffer, TFE and/or naphthalene emission as appropriate at the specific temperature and wavelength. Fluorescence units shown on figures are arbitrary fluorescence intensity units, except where spectra were scaled for comparison, in which cases appropriate ratios of them were used. In some cases spectra were scaled to the pyrene LES emission at 380 nm of the pyrene-bearing probe to facilitate visualisation of changes in the ratio between the pyrene LES and the excimer/exciplex band. The ratio between the emission intensity of the excimer/exciplex band at 480 nm and the LES band at 380 nm (I_E/I_M) was also calculated for each spectrum.

Duplex formation

1 mL volume. The complex was formed by sequential addition of aliquots (2.5 µL) of the components from stock solutions (1 mM) to Tris buffer (1 mL of 10 mM Tris, pH 8.30, 100 mM NaCl) containing the appropriate amount of TFE (0–80%) at 10 °C. Components (molar ratio 1 : 1 : 1) were added in the order: ON1-5′-X, ON2-3′-Y, then target. The concentration of each component in the cuvette was 2.5 µM. On formation of the full complex, the system was allowed to equilibrate for 10 min at 10 °C or 5 °C, and emission spectra then recorded at 3 min intervals. For the heating–re-cooling cycle, the cuvette containing all components was heated to to 70 °C for 5 min and allowed to cool back to 10 °C over 40 min. Emission spectra were then recorded at 3 min intervals until exciplex emission did not increase further (this usually occurred after 9 min). All spectra were baseline- and TFE-corrected. As the emission from naphthalene is a broad band (λ_{max} 436 nm), spectra were recorded separately for systems containing a naphthalene-bearing probe: the potential naphthalene contribution was thus shown to be very small under the conditions of excitation used.

100 µL volume. Studies were carried out to show that the types of measurement described above for 1 mL reaction volumes could also be used for smaller samples. The emission spectrum

of the full SP-19 system (ON1-5′Pyr + ON2-3′NmeNp + 16-mer oligonucleotide target) was recorded for a 1 mL sample in the cuvette (excitation 350 nm, 5 nm slitwidth, medium PMT detector voltage). An aliquot (50 µL) of this solution was pipetted into a microcuvette and the emission spectrum recorded under the same conditions, but with a high PMT detector voltage. The experiment was repeated several times, and similar spectral results were always obtained with both sample volumes (data not shown). Duplex formation was also studied on small volumes as follows. The complex was formed by sequential addition of aliquots (1.25 µL) of the components from stock solutions (0.2 mM) to Tris buffer (100 µL of 10 mM Tris, pH 8.40, 100 mM NaCl) containing the appropriate amount of TFE (0–80% v/v) at 5 °C. Components (molar ratio 1 : 1 : 1) were added in the order: ON1-5′Pyr, ON2-3′NMeNp, then target. The final concentration of each component in the cuvette was 2.5 µM. On formation of the full complex, the system was allowed to equilibrate for 5–10 min at 5 °C, and emission spectra recorded at 3 min intervals. The cuvette was then heated to 60 °C for 5 min and allowed to cool back to 5 °C over 40 min. Emission spectra were then recorded at 3 min intervals until exciplex emission did not increase further (this usually occurred after 9 min). If an exciplex emission peak at ~480 nm was not seen within this time frame, recording was extended for up to 30 min.

Melting temperature studies

Optical melting curves of the complexes were obtained using a Varian Cary 1E UV-visible spectrophotometer using a 1 mL optical cell (pathlength 1.0 cm). Thermal denaturation (T_m) measurements, detected at 260 nm and accurate to ±0.1 °C, were performed at 2.5 µM component concentrations of the 1 : 1 : 1 complex in 80% TFE–Tris buffer (10 mM Tris, pH 8.3, 100 mM NaCl). Melting data were also obtained from fluorescence emission spectra: the sample was heated to 60 °C at 0.25 °C min^{-1}. Wavelengths used were as follows: pyrene LES, λ_{ext} 340nm, λ_{em} 376 nm; exciplex band λ_{ext} 350 nm, λ_{em} 480 nm). Recordings were made at 0.5 °C increments. The sample was cooled (0.13 °C per min) and emission spectra again recorded. The melting curve obtained during cooling was used determine T_m, calculated either as the point at half the curve height[41] or by derivative calculation[42,43] using the Cary software.

References

1 E. V. Bichenkova, A. Sardarian, H. E. Savage, C. Rogert and K. T. Douglas, *Assay Drug Develop. Technol.*, 2005, **3**, 39–46.
2 K. Ebata, M. Masuko, H. Ohtani and M. Jibu, *Nucleic Acids Symp. Ser.*, 1995, **34**, 187–188.
3 K. Ebata, M. Masuko, H. Ohtani and M. Kashiwasake-Jibu, *Photochem. Photobiol.*, 1995, **62**, 836–839.
4 M. Masuko, S. Ohuchi, K. Sode, H. Ohtani and A. Shimadzu, *Nucleic Acids Symp. Ser.*, 1998, **39**, 111–112.
5 M. Masuko, H. Ohtani, K. Ebata and A. Shimadzu, *Nucleic Acids Res.*, 1998, **26**, 5409–5416.
6 M. Masuko, K. Ebata and H. Ohtani, *Nucleic Acids Symp. Ser.*, 1996, **35**, 165–166.
7 A. Shimadzu, H. Ohtani, S. Ohuchi, K. Sode and M. Masuko, *Nucleic Acids Symp. Ser.*, 1998, **39**, 45–46.
8 P. L. Paris, J. M. Langenhan and E. T. Kool, *Nucleic Acids Res.*, 1998, **26**, 3789–3793.
9 J. B. Birks, *Organic Molecular Photophysics*, Wiley, London, 1973, vol. 1.
10 J. B. Birks, *Photophysics of Aromatic Molecules*, Wiley, London, 1970.
11 H. Kashida, H. Asanuma and M. Komiyama, *Chem. Commun.*, 2006, 2768–2770.
12 E. V. Bichenkova, H. E. Savage, A. R. Sardarian and K. T. Douglas, *Biochem. Biophys. Res. Commun.*, 2005, **332**, 956–964.
13 H. Kashida, M. Komiyama and H. Asanuma, *Chem. Lett.*, 2006, **35**, 934–935.
14 D. Rehm and A. Weller, *Z. Phys. Chem. (Munich)*, 1970, **69**, 183–200.
15 S. Masaki, T. Okada, N. Mataga, Y. Sakata and S. Misumi, *Bull. Chem. Soc. Jpn.*, 1976, **49**, 1277–1283.
16 A. M. Swinnen, M. Van der Auweraer and F. C. De Schryver, *J. Photochem.*, 1985, **28**, 315–327.
17 Ph. Van Haver, N. Helsen, S. Depaemelaere, M. Van der Auweraer and F. C. De Schryver, *J. Am. Chem. Soc.*, 1991, **113**, 6849–6857.
18 A. M. Swinnen, M. Van der Auweraer, F. C. De Schryver, K. Nakatami, T. Okada and N. Mataga, *J. Am. Chem. Soc.*, 1987, **109**, 321–330.
19 T. Okada, T. Saito, N. Mataga, Y. Sakata and S. Misumi, *Bull. Chem. Soc. Jpn.*, 1977, **50**, 331–336.
20 T. Okada, T. Fujita, M. Kubota, S. Masaki and N. Mataga, *Chem. Phys. Lett.*, 1972, **14**, 563–568.
21 N. Mataga, *Pure Appl. Chem.*, 1984, **56**, 1255–1268.
22 J. W. Verhoeven, T. Scherer and R. J. Willemse, *Pure Appl. Chem.*, 1993, **65**, 1717–1722.
23 J. W. Verhoeven, *Pure Appl. Chem.*, 1990, **62**, 1585–1596.
24 M. Van der Auweraer, L. Viaene, Ph. Van Haver and F. C. De Schryver, *J. Phys. Chem.*, 1993, **97**, 7178–7184.
25 F. D. Lewis and B. E. Cohen, *J. Phys. Chem.*, 1994, **98**, 10591–10597.
26 U. Werner and H. Staerk, *J. Phys. Chem.*, 1995, **99**, 248–254.
27 E. V. Bichenkova, A. R. Sardarian, A. N. Wilton, P. Bonnet, R. A. Bryce and K. T. Douglas, *Org. Biomol. Chem.*, 2006, **4**, 367–378.
28 F. Winnik, *Chem. Rev.*, 1993, **93**, 587–614.
29 M. Ramirez-Alvarado, F. J. Blanco and L. Serrano, *Nat. Struct. Biol.*, 1996, **3**, 604–612.
30 F. J. Blanco, M. A. Jimenez, A. Pineda, M. Rico, J. Santoro and J. L. Nieto, *Biochemistry*, 1994, **33**, 6004–6014.
31 G. S. Beddard and R. S. Davidson, *J. Photochem.*, 1973, **1**, 491–495.
32 T. Okada, M. Migita, N. Mataga, Y. Sakata and S. Misumi, *J. Am. Chem. Soc.*, 1981, **103**, 4715–4720.
33 E. V. Bichenkova, D. Marks, M. I. Dobrikov, V. V. Vlassov, G. A. Morris and K. T. Douglas, *J. Biomol. Struct. Dyn.*, 1999, **17**, 193–211.
34 E. V. Bichenkova, D. S. Marks, S. G. Lokhov, M. I. Dobrikov, V. V. Vlassov and K. T. Douglas, *J. Biomol. Struct. Dyn.*, 1997, **15**, 307–320.
35 J. M. L. Pieters, R. W. W. Mans, H. van den Elst, G. A. van der Marel, J. H. van Boom and C. Altona, *Nucleic Acids Res.*, 1989, **17**, 4551–4565.
36 J. Kypr, J. Chladkova, M. Zimulova and M. Vorlickova, *Nucleic Acids Res.*, 1999, **27**, 3466–3473.
37 H. Rau and F. Totter, *J. Photochem. Photobiol., A*, 1992, **63**, 337–347.
38 H. Knibbe, *J. Chem. Phys.*, 1967, **47**, 1184–1185.
39 M. Gordon and W. R. Ware, *The Exciplex*, Academic Press, New York/San Francisco/London, 1975.
40 O. B. Ptitsyn, *FEBS Lett.*, 1981, **131**, 197–202.
41 T. M. Davis, L. McFail-Isom, E. Keane and L. D. Williams, *Biochemistry*, 1998, **37**, 6975–6978.
42 I. Kutyavin, V. S. G. Lokhov, I. A. Afonina, R. Dempcy, A. A. Gall, V. Gorn, V. E. Lukhtanov, M. Metcalf, A. Mills, M. W. Reed, S. Sanders, I. Shishkina and M. J. Vermeulen Nicolaas, *Nucleic Acids Res.*, 2002, **30**, 4952–4959.
43 T. Xia, J. SantaLucia, Jr, M. E. Burkard, R. Kierzek, S. J. Schroeder, X. Jiao, C. Cox and D. H. Turner, *Biochemistry*, 1998, **37**, 14719–14735.

This journal is © The Royal Society of Chemistry 2007

Org. Biomol. Chem., 2007, **5**, 1039–1051 | 1051